

# Protein kinase C inhibitor enzastaurin induces in vitro and in vivo antitumor activity in Waldenström macroglobulinemia

Anne-Sophie Moreau,<sup>1,2,3</sup> Xiaoying Jia,<sup>1</sup> Hai T. Ngo,<sup>1</sup> Xavier Leleu,<sup>1,2,3</sup> Garrett O'Sullivan,<sup>1</sup> Yazan Alsayed,<sup>4</sup> Alexey Leontovich,<sup>5</sup> Klaus Podar,<sup>1,2</sup> Jeffrey Kutok,<sup>1,2</sup> John Daley,<sup>1</sup> Suzan Lazo-Kallanian,<sup>1</sup> Evdoxia Hatjiharissi,<sup>1,2</sup> Marc S. Raab,<sup>1,2</sup> Lian Xu,<sup>1</sup> Steven P. Treon,<sup>1,2</sup> Teru Hideshima,<sup>1,2</sup> Kenneth C. Anderson,<sup>1,2</sup> and Irene M. Ghobrial<sup>1,2</sup>

<sup>1</sup>Dana-Farber Cancer Institute, Boston, MA; <sup>2</sup>Harvard Medical School, Boston, MA; <sup>3</sup>Service des maladies du sang, Faculté de Médecine de Lille, Centre Hospitalier Régional Universitaire de Lille, France; <sup>4</sup>Department of Internal Medicine, University of Pittsburgh, PA; <sup>5</sup>Mayo Clinic College of Medicine, Rochester, MN

**Waldenström macroglobulinemia (WM) is an incurable lymphoplasmacytic lymphoma with limited options of therapy. Protein kinase C $\beta$  (PKC $\beta$ ) regulates cell survival and growth in many B-cell malignancies. In this study, we demonstrate up-regulation of PKC $\beta$  protein in WM using protein array techniques and immunohistochemistry. Enzastaurin, a PKC $\beta$  inhibitor, blocked PKC $\beta$  activity and induced a significant decrease of proliferation at 48 hours in WM cell lines (IC<sub>50</sub>, 2.5-10  $\mu$ M). Similar effects were demonstrated in primary CD19<sup>+</sup> WM cells, with-**

**out cytotoxicity on peripheral blood mononuclear cells. In addition, enzastaurin overcame tumor cell growth induced by coculture of WM cells with bone marrow stromal cells. Enzastaurin induced dose-dependent apoptosis at 48 hours mediated via induction of caspase-3, caspase-8, caspase-9, and PARP cleavage. Enzastaurin inhibited Akt phosphorylation and Akt kinase activity, as well as downstream p-MARCKS and ribosomal p-S6. Furthermore, enzastaurin demonstrated additive cytotoxicity in combination with bortezomib, and syner-**

**gistic cytotoxicity in combination with fludarabine. Finally, in an in vivo xenograft model of human WM, significant inhibition of tumor growth was observed in the enzastaurin-treated mice ( $P = .028$ ). Our studies therefore show that enzastaurin has significant antitumor activity in WM both in vitro and in vivo, providing the framework for clinical trials to improve patient outcome in WM. (Blood. 2007;109:4964-4972)**

© 2007 by The American Society of Hematology

## Introduction

Waldenström macroglobulinemia (WM) is a low-grade lymphoplasmacytic lymphoma characterized by bone marrow infiltration with the malignant clone and symptoms related to hyperviscosity due to elevated immunoglobulin M protein in the circulation.<sup>1,2</sup> Current treatment options in WM include alkylating agents (eg, chlorambucil), nucleoside analogues (cladribine or fludarabine), and the monoclonal antibody rituximab.<sup>3,4</sup> However, WM remains incurable, and most patients eventually relapse, with a median overall survival of 5 to 6 years. Response rates in relapsed/refractory patients are 30% to 40%, with a median duration of response of only one year. In addition, most agents used in the treatment of WM have been used due to their activity in other lymphoplasmacytic disorders, and without preclinical studies showing specific activity in WM. Therefore, there is an urgent need for the development of rationally designed novel therapeutic agents targeting aberrant molecular pathways in WM.

The serine-threonine protein kinase C (PKC) family is composed of at least 11 members that mediate multiple physiological functions including differentiation, growth and survival, invasiveness, and angiogenesis.<sup>5</sup> Dysregulation of PKC signaling pathways has been implicated in tumor progression, notably B-cell lymphoma.<sup>6</sup> Specifically, PKC $\beta$  mediates growth and survival of diffuse large B-cell lymphoma,<sup>7</sup> cell proliferation in chronic lymphoid leukemia,<sup>8</sup> as well as migration and cell growth in multiple myeloma.<sup>9</sup>

Enzastaurin an acyclic bisindolylmaleimide, is a PKC $\beta$ -selective inhibitor. Enzastaurin suppresses not only PKC signaling,

but also the PI3 kinase/Akt pathway, cascades that mediate tumor-induced angiogenesis, as well as tumor cell survival and proliferation.<sup>10,11</sup> Enzastaurin also inhibits vascular endothelial growth factor (VEGF)-induced angiogenesis in animal models, suggesting that it suppresses tumor growth through multiple mechanisms.<sup>12</sup> Enzastaurin is currently being tested in phase 2 clinical trials in pancreatic, colonic, and non-small cell lung carcinoma, as well as in phase 3 clinical trials for the treatment of refractory glioblastoma and diffuse large B-cell lymphoma.

In this study, we show that PKC $\beta$  protein expression is up-regulated in WM. Of importance, down-regulation of PKC $\beta$  by enzastaurin leads to significant inhibition of proliferation and induction of apoptosis of WM cell lines and patient cells. Enzastaurin inhibits phosphorylation of PKC $\beta$  and induces caspase activation and PARP cleavage, leading to apoptosis. It also demonstrates in vivo cytotoxicity in a xenograft model of human WM in immunodeficient mice. These preclinical studies provide the basis for clinical trials of enzastaurin in WM.

## Materials and methods

### Cells

The WM cell lines (BCWM.1 and WSU-WM) and IgM-secreting low-grade lymphoma cell lines (MEC-1, RL) were used in this study. The

Submitted October 26, 2006; accepted January 31, 2007. Prepublished online as *Blood* First Edition Paper, February 6, 2007; DOI 10.1182/blood-2006-10-054577.

The publication costs of this article were defrayed in part by page charge

payment. Therefore, and solely to indicate this fact, this article is hereby marked "advertisement" in accordance with 18 USC section 1734.

© 2007 by The American Society of Hematology

BCWM.1 is a recently described WM cell line that has been developed from a patient with untreated IgM kappa WM. The cells express the typical lymphoplasmacytic phenotype. Karyotypic and multiplex fluorescent in situ hybridization (M-FISH) studies did not demonstrate cytogenetic abnormalities in this cell line.<sup>13</sup> WSU-WM<sup>14</sup> was a kind gift from Dr Al Katib (Wayne State University, Detroit, MI). MEC-1 was a kind gift from Dr Kay (Mayo Clinic, Rochester, MN). RL was purchased from the American Tissue Culture Collection (Manassas, VA). All cell lines were cultured in RPMI-1640 containing 10% fetal bovine serum (FBS; Sigma Chemical, St Louis, MO), 2 mM L-glutamine, 100 U/mL penicillin, and 100 µg/mL streptomycin (GIBCO, Grand Island, NY).

Patient samples were obtained after approval from the Dana-Farber Cancer Institute institutional review board (DFCI IRB). Informed consent was obtained from all patients according to the Declaration of Helsinki protocol. Primary WM cells were obtained from bone marrow (BM) samples using CD19<sup>+</sup> microbead selection (Miltenyi Biotec, Auburn, CA) with more than 90% purity as confirmed by flow cytometric analysis with monoclonal antibody reactive to human CD20-PE (BD Biosciences, San Jose, CA). Peripheral blood mononuclear cells (PBMCs) were obtained from healthy volunteers by Ficoll-Hypaque density sedimentation. Bone marrow CD19<sup>+</sup> selected B cells from healthy donors were used as control.

## Reagents

Enzastaurin hydrochloride [1H-pyrrole-2,5-dione,3-(1-methyl-1H-indol-3-yl)-4-[1-[-(2-pyridinylmethyl)-4-piperidinyl]-1H-indol-3-yl]], LY 317615, an acyclic bisindolylmaleimide, was provided by Eli Lilly (Indianapolis, IN). Rituximab was a kind gift from S. Treon (Dana-Farber Cancer Institute, Boston, MA). Bortezomib was obtained from Millennium Pharmaceuticals (Cambridge, MA). Fludarabine and dexamethasone were purchased from Sigma (St Louis, MO). 12-Deoxyphorbol-13-phenylacetate-20-acetate (DOPPA), a specific PKCβ stimulator, was purchased from Biomol (Plymouth, PA).

## Protein microarray procedure

CD19<sup>+</sup> lymphoplasmacytic cells were selected (95% purity) with immunomagnetic beads (Miltenyi Biotec) from BM of 5 patients with WM and 3 healthy individuals after informed consent from the DFCI IRB-approved protocol. The nanoscale Antibody Microarray (Clontech, Mountain View, CA) contains 512 highly specific and sensitive monoclonal antibodies that detect a wide variety of proteins representing a broad range of biologic functions including signal transduction, cell-cycle regulation, gene transcription, and apoptosis. The complete list of the arrayed antibodies is available at <http://bioinfo2.clontech.com/abinfo/array-list-action.do>. The technique was performed as previously described.<sup>15</sup> Labeling the proteins from both normal and malignant B cells with Cy3 and Cy5 allowed for microarray detection of differences in specific protein abundance between the WM and control samples. The slides were scanned using Axon GenePix 4000B scanner (Molecular Devices, Sunnyvale, CA), as previously described. The mean of the Cy5/Cy3 ratios of both slides was analyzed using Clontech Excel software. The Genespring software (Silicon Genetics, Redwood City, CA) was used for analysis of all 5 experiments and normalized to controls. An unsupervised clustering analysis was performed to identify changes that were 2-fold or 1.3-fold or higher in at least 3 (67%) of 5 WM samples compared to the control.

## Histologic examination of BM biopsies

BM trephine biopsies from the same samples used for protein microarrays were fixed in neutral-buffered formalin and processed into paraffin wax-embedded blocks for histology by standard methods. Sections were cut at 4 µm and floated onto Colorfrost/Plus electrostatically prepared precleaned slides (Fisher Scientific, Hampton, NH) to ensure adhesion. Initial morphologic assessment was done after hematoxylin and eosin (H&E) staining. Immunoperoxidase studies were performed using an indirect technique, as previously described,<sup>16</sup> with modifications. Mouse antibody to human PKCβ was obtained from BD Biosciences, and swine anti-mouse Ig conjugated to horseradish peroxidase was obtained from

Dako (Carpinteria, CA). Antibody localization was effected using a peroxidase reaction with 3,3-diaminobenzidine tetrahydrochloride as chromogen and detected using the Envision Plus detection system (Dako). Slides were counterstained with Harris hematoxylin and examined by standard light microscopy. Samples were analyzed using an Olympus BX41 microscope equipped with a UPlan FL 40 ×/0.75 numerical aperture (NA) or a 20 ×/0.50 NA objective lens (Olympus, Melville, NY). Pictures were taken using Olympus QColor3 and analyzed using QCapture 2.60 software (QImaging, Burnaby, BC).

## Lentivirus shRNA vector construction

To further determine the role of PKCβ in the regulation of apoptosis in WM, we used shRNA sequences to knock down PKCβ in BCWM.1 cell line using a lentivirus transfection system.<sup>18,19</sup> The shRNA was kindly provided by The RNAi Consortium (RTC) of Dana-Farber Cancer Institute, and the sense oligonucleotide sequence for construction of PKCβ gene (*PRKCB*) shRNAs was as follows: clone no. 1, *PRKCB1*: target sequence 5'-CTATCCCAAGTCTATGTCCAA-3'; clone no. 2, *PRKCB1*: target sequence 5'-GCTGAAAGAATCGGACAAAGA-3'; clone no. 3, *PRKCB1*: target sequence 5'-CAAGTTTAAGATCCACACGTA-3'; clone no. 4, *PRKCB1*: target sequence 5'-CCGGTATATTGATTGGGAGAA-3'; clone no. 5, *PRKCB1*: target sequence 5'-CCGGATGAAACTGACCGATT-3'; clone no. 6, *PRKCB2*: target sequence 5'-CCAATCAGAATTTCGAAG-GATT-3'. pLKO.1 plasmid with target sequence PKCβ shRNA or pLKO.1 control plasmid was cotransfected with pVSV-G and p8.9 plasmids into 293T packaging cells with Lipofectamine 2000 (Invitrogen Life Technologies, Carlsbad, CA). BCWM.1 cells were then transduced with the culture supernatants containing the released virus mixed with equal amount of reconstituted RPMI 10% after 24 hours and 48 hours. Two days after infection, cells were analyzed for PKCβ, PARP, and β-actin expression using immunoblotting.

## Growth inhibition assay

The inhibitory effect of enzastaurin, alone or in combination with other agents, on WM cell growth was assessed by measuring 3-(4,5-dimethylthiazol-2-yl)-2,5-diphenyltetrazolium bromide (MTT; Chemicon International, Temecula, CA) dye absorbance as previously described.<sup>17</sup> Briefly, cells were seeded at a density of  $4 \times 10^4$  cells per well in a 96-well plate and treated with enzastaurin or DMSO (vehicle). MTT (10 µL) was added to each well for the last 4 hours of 24-hour and/or 48-hour cultures. Absorbance was measured at 570/630 nm using a spectrophotometer (Molecular Devices, Sunnyvale, CA). All experiments were performed in triplicate.

## DNA synthesis

WM cells ( $4 \times 10^4$  cells/well) were cultured in the presence of RPMI with 10% fetal bovine serum with enzastaurin, alone or in combination with other agents, in the presence or absence of recombinant cytokines (IL-6 and IGF-1) for 48 hours at 37°C. DNA synthesis was measured by [<sup>3</sup>H]-thymidine ([<sup>3</sup>H]-TdR; Perkin Elmer, Boston, MA) uptake, as previously described.<sup>17</sup> All experiments were performed in triplicate.

## Flow cytometry analysis

Cell-cycle analysis was performed using flow cytometry with the dye 4',6-diamidino-2-phenylindole (DAPI). Propidium iodide was not used due to interference of enzastaurin autofluorescence with the commonly used wavelengths (FL2, FL3, FL4, and FL5). Briefly, WM cells were cultured for 24 hours with enzastaurin or control media, treated with 10 µg/mL RNase (Roche Diagnostics, Indianapolis, IN), and stained with DAPI (10 µg/mL) in Triton X-100 solution (0.1% in PBS), and then cell-cycle profile was determined using an Epics Altra flow cytometer (Coulter Immunology, Hialeah, FL).

Annexin V-FITC and DAPI staining were used to detect and quantify apoptosis by flow cytometry. BCWM.1 cells ( $1 \times 10^6$  cells) were cultured in 24-well plates for 24 hours with enzastaurin (2.5 to 20 µM) or control media. Cells were then harvested in cold phosphate-buffered saline (PBS) and pelleted by centrifugation for 5 minutes at 400 g. They were then

resuspended at  $1 \times 10^6$  cells/mL in binding buffer (HEPES buffer, 10 mM, pH 7.4, 150 mM NaCl, 5 mM KCl, 1 mM  $MgCl_2$ , 1.8 mM  $CaCl_2$ ), stained with annexin V-FITC and DAPI, and incubated in the dark for 15 minutes. Cells were processed with an Epics Altra flow cytometer (Coulter Immunology).

### Immunoblotting

WM cells were harvested and lysed using lysis buffer (Cell Signaling Technology, Beverly, MA) reconstituted with 5 mM NaF, 2 mM  $Na_3VO_4$ , 1 mM PMSF, 5  $\mu$ g/mL leupeptin, and 5  $\mu$ g/mL aprotinin. Whole-cell lysates were subjected to sodium dodecyl sulfate–polyacrylamide gel electrophoresis (SDS-PAGE) and transferred to polyvinylidene fluoride membrane (Bio-Rad Laboratories, Hercules, CA). The antibodies used for immunoblotting included anti-phospho (p)-PKC $\beta$ /II (thr500; Upstate, Temecula, CA); anti-PKC $\beta$  (BD Biosciences); anti-pan-p-PKC (ser660), anti-p-Akt (Ser473), anti-Akt, anti-p-PDK1 (Ser241), anti-p-GSK3 $\alpha/\beta$  (Ser21/9), anti-p-MARCKs (ser152/156), anti-p-ERK1/2 (thr202/tyr204), anti-ERK1/2, anti-p-S6 ribosomal (ser240/244), anti-caspase-3, anti-caspase-8, anti-caspase-9, and anti-PARP (Cell Signaling Technology); and anti- $\alpha$ -tubulin (Santa Cruz Biotechnology, Santa Cruz, CA) antibodies.

### In vitro Akt kinase assay

In vitro Akt kinase assay (Cell Signaling Technology) was performed as previously described.<sup>17</sup> Briefly, BCWM.1 cells were cultured in the presence or absence of enzastaurin (5  $\mu$ M and 10  $\mu$ M for 30 and 60 minutes). Cells were subsequently lysed in  $1 \times$  lysis buffer, and lysates were immunoprecipitated with immobilized Akt primary antibody and incubated with gentle rocking overnight at 4°C. Cell lysate/immobilized antibody were microcentrifuged and pellets were washed twice with  $1 \times$  cell lysis buffer, and twice with  $1 \times$  kinase buffer. Pellets were resuspended in  $1 \times$  kinase buffer supplemented with ATP and GSK-3 fusion protein, and then incubated for 30 minutes at 30°C. Samples were run on SDS-PAGE and transferred to PVDF membrane. Kinase activity was detected by immunoblotting with phospho-GSK-3 $\alpha/\beta$  (Ser21/9) antibody (Cell Signaling Technology).

### Antibody-dependent cell-mediated cytotoxicity assay (ADCC)

ADCC was performed as previously described.<sup>20</sup> Briefly, interleukin-2 (IL-2; R&D, Minneapolis, MN)-activated PBMCs were used as effector cells and calcein-AM-labeled BCWM.1 cell line, as targets. PBMCs were separated from leukopheresis products from healthy donors over Ficoll-Hypaque solution (density = 1.077 g/L) after informed consent. Effector cells were used immediately at 37°C in RPMI complete media after being activated with IL-2 (100 U/mL for 36 hours). Target cells were labeled with calcein-AM for 1 hour at 37°C, washed thrice, and plated in triplicate in 96-well plates (5000 cells per well). ADCC was performed in the presence of rituximab (10  $\mu$ g/mL) or human control IgG1 (2  $\mu$ g/mL) at various effector-target (E/T) ratios (10:1, 20:1, and 40:1). The 96-well plates were centrifuged at 30 g for 2 minutes at room temperature, followed by a 4-hour incubation at 37°C. Culture supernatants were transferred to a Black ViewPlate-96 plate and read on Wallac VICTOR2 using 492/520 nm filter set (Perkin Elmer). This assay was valid only if (mean maximum release – medium control release)/(mean spontaneous release – medium control release) was more than 7. Spontaneous release is the CPM in the supernatant from wells containing target cells alone. Maximum release is the supernatants of wells containing target cells and Triton X-100. Experimental release is obtained from the supernatant of wells containing effector cells, target cells, and antibody. Calculation of percentage specific lysis from triplicate experiments was done using the following equation: % specific lysis =  $100 \times [(\text{mean experimental release} - \text{mean spontaneous release}) / (\text{mean maximum release} - \text{mean spontaneous release})]$ . Experiments were also done in which target WM cells were treated with both enzastaurin (7.5  $\mu$ M overnight) and rituximab (10  $\mu$ g/mL) before ADCC. All cells were counted and assessed for viability (> 90%) by means of trypan blue staining before ADCCs. Cells were suspended in complete media and plated at E/T ratios of 40:1, 20:1, 10:1, and 0:1.

### Colony-forming unit assay (CFU assay)

CFU assays were performed in the presence or absence of enzastaurin (15  $\mu$ M and 20  $\mu$ M) in Iscove modified Dulbecco medium (IMDM) supplemented with 1% methylcellulose, 30% FBS, 1% bovine serum albumin, 2 mM L-glutamine, plus recombinant human erythropoietin (3 U/mL), IL-3 (10 ng/mL), stem cell factor (50 ng/mL), and GM-CSF (10 ng/mL). Semisolid cultures were performed in duplicates. Hematopoietic colonies were enumerated with an inverted microscope. Approximately  $5 \times 10^3$  cells were cultured, and colonies (burst-forming units–erythroid [BFU-Es], colony-forming units–granulocyte-macrophage [CFU-GMs], colony-forming units–macrophage [CFU-Ms], and colony-forming units–granulocyte-macrophage-erythroid-megakaryocyte [CFU-GEMMs]) were counted at day 14.

### Effect of enzastaurin on paracrine WM cell growth in the BM

To evaluate growth stimulation and signaling in WM cells adherent to bone marrow stromal cells (BMSCs),  $3 \times 10^4$  BCWM.1 cells were cultured in BMSC-coated 96-well plates for 48 hours in the presence or absence of enzastaurin. DNA synthesis was measured as previously described.<sup>17</sup>

### Xenograft murine model

Severe combined immunodeficient (SCID) homozygous female mice NIH III (5 weeks old) were obtained from Charles River Lab (Wilmington, MA) and irradiated. All animal studies were conducted according to protocols approved by the Animal Ethics Committee of the Dana-Farber Cancer Institute. The mice were inoculated subcutaneously in the right flank with  $3 \times 10^6$  BCWM.1 cells in 100  $\mu$ L PBS. Once tumors were measurable, mice were assigned into cohorts receiving either oral gavage with enzastaurin suspended in dextrose 5% in water according to the company's instructions (80 mg/kg twice daily; n = 9) or oral vehicle alone (n = 6). Caliper measurements of the longest perpendicular tumor diameters were performed every alternate day to estimate the tumor volume, using the following formula representing the 3-dimensional volume of an ellipse:  $4\pi/3 \times (\text{width}/2)^2 \times (\text{length}/2)$ . Tumor growth was evaluated from the first day of treatment until 1 of the 2 groups reached significant involvement in tumor. Animals were killed and protein expression within tumor was analyzed.

### Statistical analysis

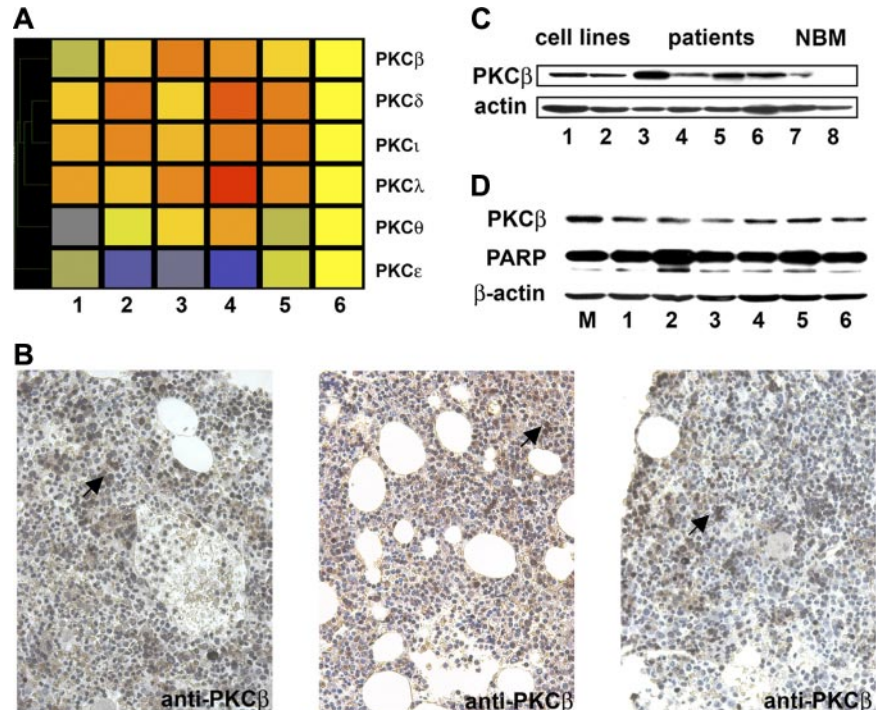
Statistical significance of differences observed in drug-treated versus control cultures was determined using Student *t* test. The minimal level of significance was  $P < .05$ . The interaction between enzastaurin and bortezomib and fludarabine was analyzed by isobologram analysis using the CalcuSyn software program (Biosoft, Ferguson, MO) to determine if the combinations were additive or synergistic. The Chou-Talalay method, the basis for this program, calculates a combination index (CI) to indicate additive or synergistic effects. When CI = 1, effects are additive. When CI is less than 1.0, effects are synergistic. Results from viability assays (MTT) were expressed as fraction of cells killed by the individual drugs or the combination in drug-treated versus untreated cells. For in vivo experiments, tumor volumes were compared using 1-way analysis of variance and Bonferroni posthoc tests.

## Results

### PKC $\beta$ is elevated in patients with WM and is essential for the survival of WM cells

Using the nanoscale protein array, we found 72 proteins up- or down-regulated by 1.3-fold in WM samples compared to control. These included PKC family proteins PKC $\beta$ , PKC $\delta$ , PKC $\gamma$ , and PKC $\iota$  (Figure 1A); proteins in the PI3K pathway such as VHR, PTP1B, PI3K (p110alpha), and Rb2; B-cell-specific activator protein PAX-5; the phospholipase protein PLC $\gamma$ ; the ubiquitin protein UBCH6; the STAT kinase STAT4; the GTPase Rho A-binding kinase ROK $\alpha$ ; and the apoptosis protein SMAC/

**Figure 1. PKC $\beta$  is elevated in patients with WM and is essential for the survival of WM cells.** (A) Proteomic analysis of some PKC protein family members: the WM samples are numbered 1 to 5. The control sample (composed of 3 control samples mixed) is at the far right of the heat map. All the samples were normalized to the control sample using the Genespring software. The data points are colored by expression with lower signal values colored blue and higher values, red. Yellow signifies expression values equal to the control sample. (B) Immunohistochemistry with anti-PKC $\beta$  on patient's bone marrow biopsy demonstrating increased staining in the WM samples 2, 3, and 4 of the protein microarrays. The arrows indicate some examples of PKC $\beta$ -positive cells. (C) Whole-cell lysates from BCWM.1 (1), MEC1 (2), as well as 4 patients' bone marrow samples CD19 $^+$  selected (3 to 6) and 2 healthy donors' bone marrows CD19 $^+$  selected (7 and 8) were subjected to Western blotting using anti-PKC $\beta$  antibody.  $\beta$ -Actin was used as control. PKC $\beta$  was overexpressed in WM samples compared to control. (D) BCWM.1 cells were transfected with 6 different shRNAs (1 to 6) or mock (M) using a lentivirus transfection system. At 48 hours after transduction, whole-cell lysates were subjected to Western blotting using anti-PKC $\beta$ , anti-PARP, and anti- $\beta$ -actin antibodies.



DIABLO (data not shown). We confirmed our results by immunohistochemistry with anti-PKC $\beta$  antibody staining on WM bone marrow samples (2, 3, and 4) used for protein microarray (Figure 1B). We next performed immunoblotting for PKC $\beta$  in BM CD19 $^+$  selected cells from 3 patients with WM, BM CD19 $^+$  cells from 2 healthy donors, as well as BCWM.1 and MEC1 cell lines. Baseline expression of PKC $\beta$  was increased in BM CD19 $^+$  patients' samples compared to normal BM CD19 $^+$  cells (Figure 1C). In addition, to determine the effect of inhibition of PKC $\beta$  on the survival of WM cells, we used specific PKC $\beta$  shRNA sequences to knock down PKC $\beta$  expression in BCWM.1. As shown in Figure 1D, PKC $\beta$  was partially inhibited with the different shRNAs. This led to induction of apoptosis in the PKC $\beta$  knockdown cells compared to mock-infected cells as demonstrated by PARP cleavage. These data indicate that PKC $\beta$  is essential for the survival of WM cells.

#### Enzastaurin blocks proliferation in WM cells and induces cytotoxicity

WM and IgM-secreting cell lines next were cultured for 24, 48, and 72 hours in the presence of enzastaurin (2.5 to 20  $\mu$ M). As shown in Figure 2A, enzastaurin inhibited BCWM.1 proliferation at 48 and 72 hours, as measured by  $^3$ H-thymidine uptake assay, with an IC $_{50}$  between 5 and 7.5  $\mu$ M (Figure 2A). Enzastaurin demonstrated similar activity on all cell lines tested, with IC $_{50}$  between 5 and 15  $\mu$ M at 48 hours as shown in Figure 2B.

We then studied the cytotoxic effect of enzastaurin (2.5 to 20  $\mu$ M) on cell lines and WM patient cells by MTT assay. Enzastaurin decreased survival of BCWM.1 cells (IC $_{50}$ , 10  $\mu$ M; Figure 2C) and other IgM-secreting cell lines (IC $_{50}$ , 7.5-20  $\mu$ M; Figure 2D), and was confirmed in tumor cells from patients ( $n = 3$ ; Figure 2E). In contrast, enzastaurin had no cytotoxic effect on PBMCs from 3 healthy volunteers (Figure 2F) or on BM hematopoietic progenitor cells (Figure 2G). These results demonstrate that enzastaurin triggers significant cytotoxicity in tumor cell lines and patient WM cells, without toxicity in normal PBMCs.

#### Enzastaurin induces apoptosis in WM cells

We next examined the molecular mechanisms whereby enzastaurin induces cytotoxicity in WM cells. We demonstrated that enzastaurin induced time- and dose-dependent apoptosis, evidenced by annexin V and DAPI staining and flow cytometry analysis, with 10  $\mu$ M drug inducing 21% apoptosis at 48 hours in BCWM.1 cells (Figure 3A), as well as in other IgM-secreting cell lines (data not shown). To determine the mechanism of enzastaurin-induced apoptosis, we investigated the effect of enzastaurin on BCWM.1 cells using immunoblotting. Enzastaurin induced activation of the intrinsic pathway of apoptosis in a dose-dependent fashion, with caspase-9, caspase-3, and PARP cleavage at 15  $\mu$ M at 6 hours (Figure 3B). Enzastaurin induced caspase-8 and PARP cleavage in a time-dependent fashion, suggesting extrinsic pathway activation (Figure 3C), with 7.5  $\mu$ M drug inducing PARP cleavage at 4 hours and caspase-8 cleavage at 12 hours. In addition, as shown in Figure 3D, enzastaurin (2.5  $\mu$ M to 10  $\mu$ M) had no effect on cell-cycle profile, but 10  $\mu$ M enzastaurin induced apoptosis with 35% sub-G $_0$ /G $_1$  cells at 24 hours.

#### Signaling pathways regulated by enzastaurin

Enzastaurin inhibited phosphorylation of PKC $\beta$  and pan-phospho-PKC in a dose-dependent fashion, as shown in Figure 4A. In a time- and dose-dependent fashion, enzastaurin also inhibited phosphorylation of proteins downstream of PKC $\beta$  including the specific PKC substrate MARCKS (myristoylated alanine-rich protein kinase C substrate), GSK3 $\beta$ , and ribosomal S6 kinase (Figure 4B-C).

Previous studies have demonstrated that Akt is downstream of PKC activation. Here we demonstrated that enzastaurin inhibits Akt phosphorylation in a time-dependent fashion, with near total inhibition at 1 hour (Figure 4C). Akt kinase activity assay decreased phosphorylation of GSK3 fusion protein after treatment with enzastaurin (7.5  $\mu$ M) at 30 and 60 minutes (Figure 4D).

We next investigated the effect of enzastaurin on the MEK/ERK pathway, which is activated in response to Akt inhibition.<sup>17</sup> As expected,

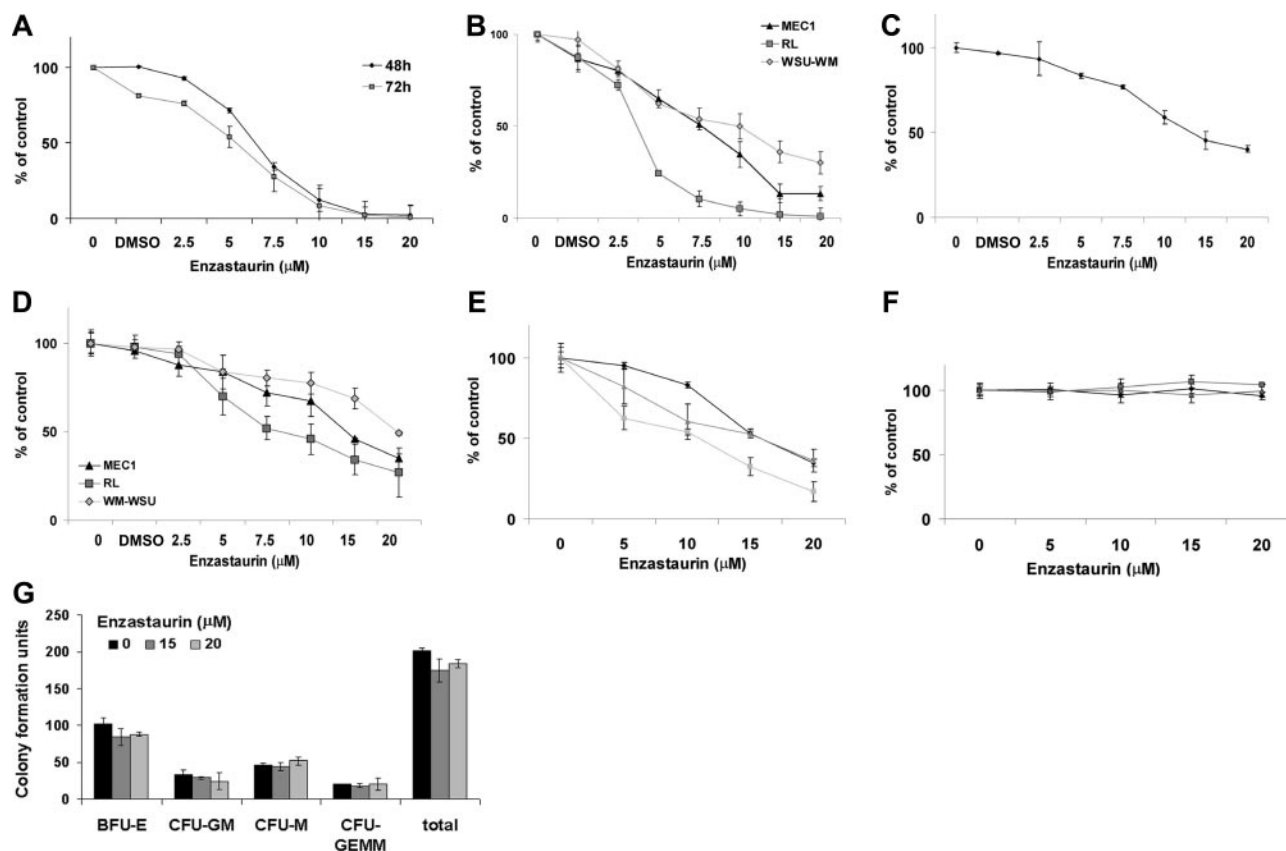


**Figure 2. Enzastaurin induced a decrease in proliferation and triggers cytotoxicity.** (A) Thymidine uptake assay. BCWM.1 was cultured with enzastaurin (2.5 to 20  $\mu\text{M}$ ) or solvent control (DMSO) for 48 hours (●) and 72 hours (◻). (B) Thymidine uptake assay. Several IgM-secreting cell lines, RL, MEC-1, and WM-WSU, were cultured with enzastaurin (2.5 to 20  $\mu\text{M}$ ) solvent control (DMSO). (C) BCWM.1 cells were cultured with enzastaurin (2.5 to 20  $\mu\text{M}$ ) solvent control (DMSO) for 48 hours. Cytotoxicity was assessed by MTT assay. (D) Several IgM-secreting cell lines, RL, MEC-1, and WM-WSU, were cultured with enzastaurin (2.5 to 20  $\mu\text{M}$ ) solvent control (DMSO) for 48 hours. Cytotoxicity was assessed by MTT assay. (E-F) Freshly isolated bone marrow CD19<sup>+</sup> tumor cells from 3 patients with WM (E) and PBMCs from 3 healthy donors (F) were cultured with enzastaurin (5 to 20  $\mu\text{M}$ ). Cytotoxicity was assessed by MTT assay. (G) Colony-forming cell assay. Negative fraction after CD19<sup>+</sup> selection of bone marrow mononuclear cells was cultured using methylcellulose semisolid technique in absence and presence of enzastaurin (15 and 20  $\mu\text{M}$ ), and BFU-E, CFU-GM, CFU-M, and CFU-GEMM were counted at day 14. All results represent means ( $\pm$  SD). All experiments have been done in triplicate.

we found an increase in ERK phosphorylation in response to enzastaurin in a dose-dependent fashion (Figure 4E). Given that ERK activation protects the cells from apoptosis, we studied the effect of the MEK inhibitor U0126 with enzastaurin on proliferation, using the thymidine uptake assay. As shown in Figure 4F, the combination of enzastaurin (7.5  $\mu\text{M}$ ) and U0126 (10 nM) triggered an additive inhibition of proliferation, with a CI of 0.865 (Chou-Talalay method).

#### Neither growth factors nor adherence to BMSCs protects against enzastaurin-induced WM cell cytotoxicity

We next examined the effect of enzastaurin in the presence of a specific PKC $\beta$  stimulator, DOPPA. As shown on Figure 5A, DOPPA (200 nM) induced activation of PKC $\beta$  at 20 minutes. Even in the presence of DOPPA (200 nM), enzastaurin was able to overcome the growth stimulatory effect of DOPPA with an IC<sub>50</sub> of 5 to 7.5  $\mu\text{M}$  (Figure 5B).

Previous studies using gene expression analysis in WM have demonstrated that IL-6 signaling is up-regulated.<sup>21</sup> IL-6 also promotes plasmacytoid lymphocyte growth in WM, as well as reflects tumor burden and disease severity.<sup>21</sup> We therefore tested the effect of IL-6 on WM cells, and determined whether enzastaurin can overcome its protective effect. As shown in Figure 5C, enzastaurin (5 and 10  $\mu\text{M}$ ) was able to overcome proliferation induced by IL-6 (25 ng/mL).

Since the BM microenvironment confers growth and drug resistance in malignant cells,<sup>22,23</sup> we next studied whether enzastaurin overcomes the protective effect conferred by the BMSCs. BCWM.1 cells were cultured with enzastaurin (2.5, 5, and 7.5  $\mu\text{M}$ ), in the presence or absence of BMSCs. As shown in Figure 5D, adherence of BCWM.1 cells to BMSCs triggered a 2-fold increase in proliferation, which was inhibited by enzastaurin in a dose-dependent fashion ( $P < .001$ ). These data indicate that enzastaurin triggers significant antitumor activity in the bone marrow milieu.

#### Enzastaurin enhances cytotoxicity of other main therapeutic agents in WM

The monoclonal anti-CD20 antibody rituximab is a main therapeutic modality used in WM. We, therefore, next determined the effect of the combination of enzastaurin with rituximab, assessed by ADCC. Cytotoxicity of rituximab on BCWM.1 cells increased with increasing effector-target ratio (0:1, 10:1, 20:1, 40:1) mediating 8% to 41% specific lysis. Specific lysis increased from 41% with rituximab alone to 55% when rituximab 10  $\mu\text{g/mL}$  was combined with enzastaurin 7.5  $\mu\text{M}$  and E/T ratio of 40:1. Increased specific lysis with the combination was observed at all E/T ratios studied (Figure 6A).

We similarly determined the effects of enzastaurin in combination with bortezomib, another active agent in WM. BCWM.1 cells were cultured for 48 hours with bortezomib (5 to 10 nM) alone or in

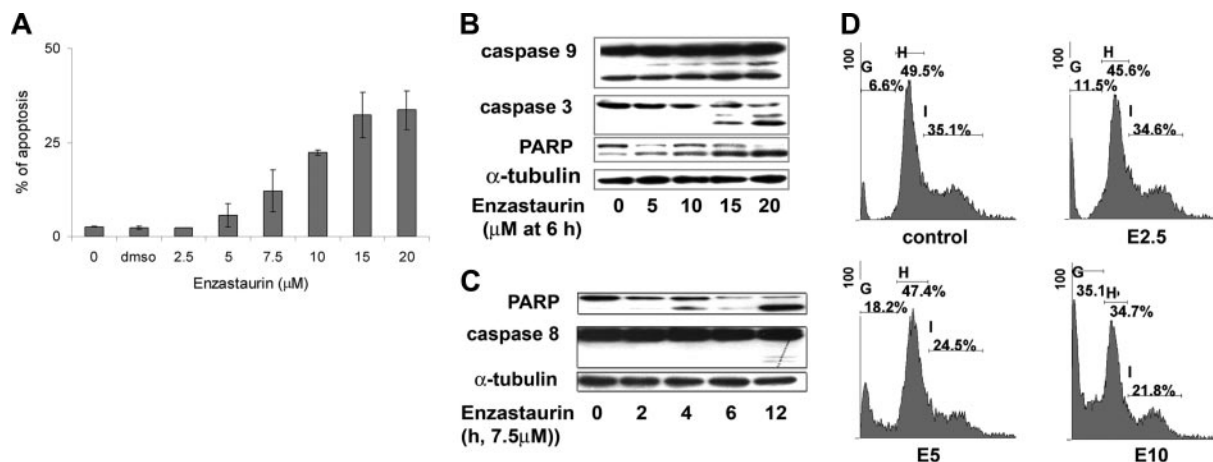


**Figure 3. Enzastaurin induced apoptosis in WM cell line BCWM.1.** (A) BCWM.1 cells were cultured with enzastaurin for 48 hours at doses that range from 2.5 to 20  $\mu\text{M}$ , and the percentage of cells undergoing apoptosis was studied by annexin V and DAPI staining at 48 hours. Annexin V- and DAPI-positive cells were considered as apoptotic. Error bars represent the result and SD of 3 different experiments. (B) BCWM.1 cells were cultured with enzastaurin (5 to 20  $\mu\text{M}$ ) for 6 hours. Whole-cell lysates were subjected to Western blotting using anti-caspase 9, anti-caspase 3, anti-PARP, and  $\alpha$ -tubulin antibodies. Enzastaurin induced a cleavage of caspases and PARP in a dose-dependent fashion. (C) BCWM.1 cells were cultured with enzastaurin (7.5  $\mu\text{M}$ ) for the indicated periods. Whole-cell lysates were subjected to Western blotting using anti-caspase 8, anti-PARP, and  $\alpha$ -tubulin antibodies. Enzastaurin induced cleavage of caspase-8 and PARP in a time-dependent fashion. (D) Cell cycle was studied using DAPI staining by flow cytometry at 24 hours with control media or enzastaurin 2.5 to 10  $\mu\text{M}$  (E2.5, E5, E10). Percentages indicate cells in sub-G<sub>0</sub>/G<sub>1</sub> phase (G), G<sub>0</sub>/G<sub>1</sub> phase (H), and G<sub>2</sub>/M phase (I).

combination with enzastaurin (2.5 to 5  $\mu\text{M}$ ). As shown in Figure 6B, bortezomib-induced cytotoxicity was significantly increased by enzastaurin in a dose-dependent fashion. Bortezomib 10 nM induced 28% cytotoxicity, which was augmented in an additive fashion to 45% (CI = 0.838) and 56% (CI = 0.757) by 2.5  $\mu\text{M}$  and 5  $\mu\text{M}$  enzastaurin, respectively. There was no difference in the cytotoxic effect of the combination of bortezomib and enzastaurin when the agents were used simultaneously or sequentially.

We also studied the combination of enzastaurin with fludarabine *in vitro*, as fludarabine is another chemotherapeutic agent commonly used in WM. BCWM.1 cells were cultured for 48 hours with fludarabine (5 to 10  $\mu\text{g/mL}$ ) alone or in combination with enzastaurin (5 to 7.5  $\mu\text{M}$ ). The IC<sub>50</sub> of fludarabine was 10  $\mu\text{g/mL}$

using the cytotoxicity assay. This dose induced 22% apoptosis using annexin/DAPI staining. Enzastaurin (5  $\mu\text{M}$ ) induced 18% cytotoxicity, which increased to 62% with fludarabine 5  $\mu\text{g/mL}$  (CI = 0.676) and to 77% with fludarabine 10  $\mu\text{g/mL}$  (CI = 0.524), indicating strong synergism (Figure 6C). Isobologram analysis confirmed that the combination of enzastaurin and fludarabine was synergistic (Figure 6D).

As dexamethasone is also widely used for WM treatment, we studied the effect of dexamethasone (50 to 100 ng/mL) alone or in combination with enzastaurin (5 to 10  $\mu\text{M}$ ). Enzastaurin (7.5  $\mu\text{M}$ ) induced 27% cytotoxicity, which was increased to 42% with dexamethasone 50 ng/mL (CI = 0.895) and to 45% with dexamethasone 100 ng/mL (CI = 0.877), indicating an additive effect (data

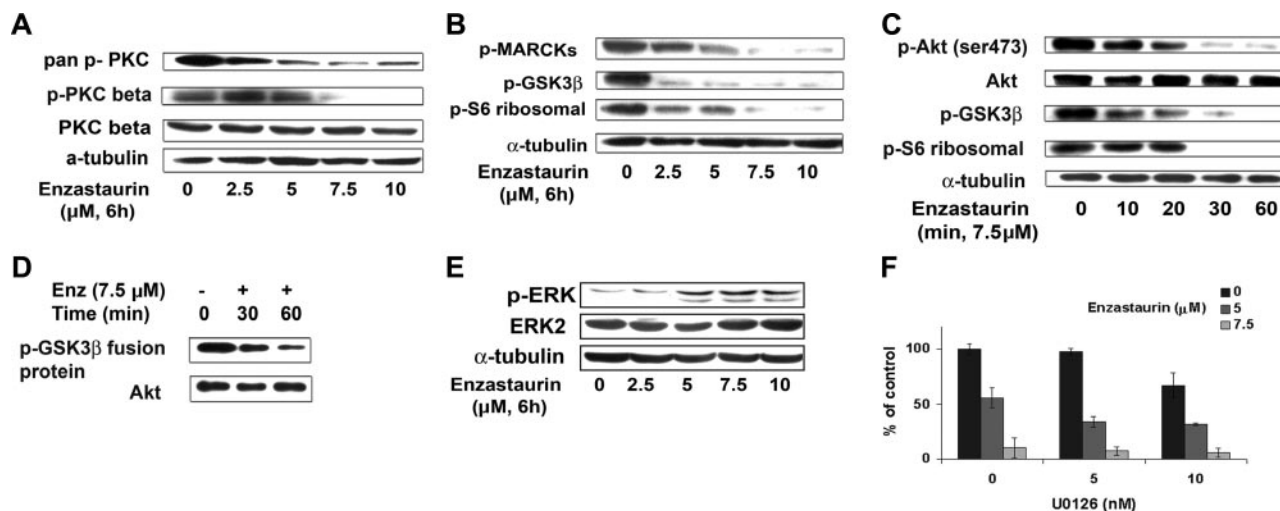


**Figure 4. Enzastaurin targets the Akt signaling pathway.** (A) BCWM.1 cells were cultured with control media or enzastaurin (2.5 to 10  $\mu\text{M}$ ) for 6 hours. Whole-cell lysates were subjected to Western blotting using anti-pan-p-PKC (ser660), anti-p-PKC $\beta$  (thr500), anti-PKC $\beta$ , and  $\alpha$ -tubulin antibodies. (B) BCWM.1 cells were cultured with control media, enzastaurin (2.5 to 10  $\mu\text{M}$ ) for 6 hours. Whole-cell lysates were subjected to Western blotting using anti-p-MARCKs, anti-p-GSK3 $\alpha/\beta$ , anti-p-S6 ribosomal, and anti- $\alpha$ -tubulin antibodies. (C) BCWM.1 cells were cultured with enzastaurin 7.5  $\mu\text{M}$  for the time indicated. Whole-cell lysates were subjected to Western blotting using anti-p-Akt, total Akt, anti-p-GSK3 $\alpha/\beta$ , anti-p-S6 ribosomal, and anti- $\alpha$ -tubulin antibodies. (D) Akt kinase assay. BCWM.1 cells were cultured with control media or enzastaurin 7.5  $\mu\text{M}$  for 30 minutes or 1 hour. Whole-cell lysates were immunoprecipitated with anti-Akt antibody, washed, and subjected to *in vitro* kinase assay according to the manufacturer's protocol. Western blotting used Akt and phospho-GSK3 $\alpha/\beta$  antibodies. (E) BCWM.1 cells were cultured with enzastaurin (2.5 to 10  $\mu\text{M}$ ) for 6 hours. Whole-cell lysates were subjected to Western blotting using anti-p-ERK, anti-ERK1/2, and  $\alpha$ -tubulin antibodies. (F) BCWM.1 cells were cultured for 48 hours with media and with enzastaurin (5 to 7.5  $\mu\text{M}$ ) in the absence or presence of 5 and 10  $\mu\text{M}$  MEK1/2 inhibitor U0126. Cytotoxicity was assessed by MTT assay. Data represent mean ( $\pm$  SD) of triplicate experiments.

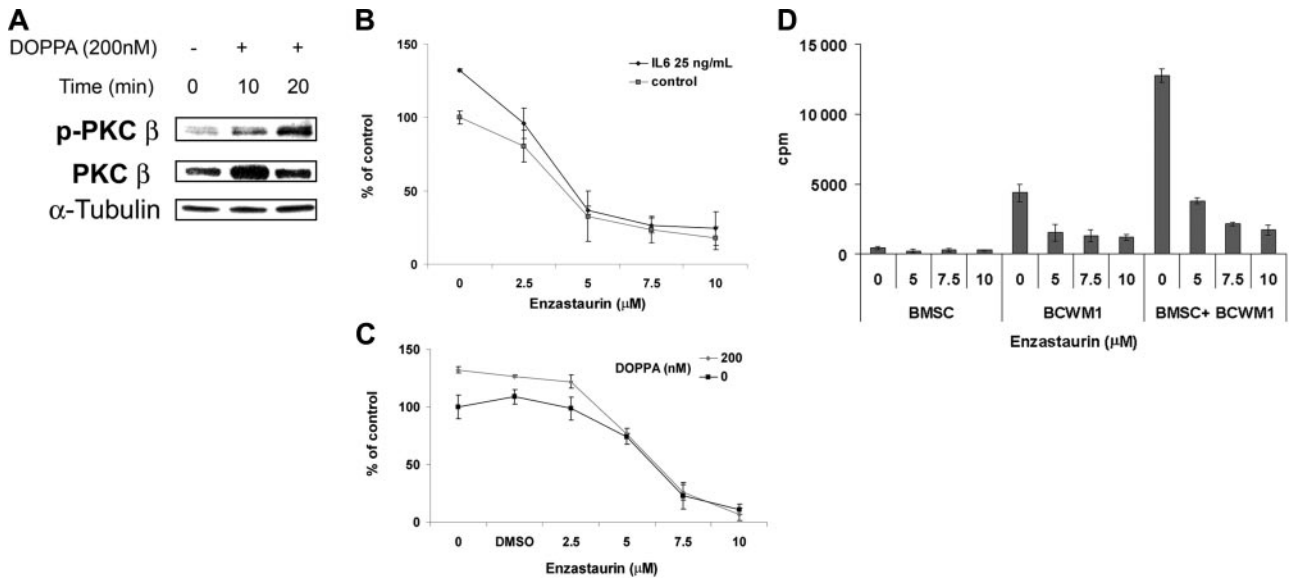


**Figure 5. Growth factors and coculture with BMSCs do not protect against enzastaurin-induced WM cell cytotoxicity.** (A) BCWM.1 cells were cultured with DOPPA (200 nM) for 10 and 20 minutes. Whole-cell lysates were subjected to Western blotting using anti-p-PKC $\beta$ , anti-PKC $\beta$ , and  $\alpha$ -tubulin antibodies. (B) BCWM.1 cells were cultured with control media in the absence and presence of DOPPA (200 nM) and treated with enzastaurin (2.5 to 10  $\mu$ M) for 48 hours. Inhibition of proliferation was assessed by thymidine uptake assay. (C) BCWM.1 cells were cultured with control media, and with 5  $\mu$ M, 7.5  $\mu$ M, and 10  $\mu$ M enzastaurin for 48 hours, in the presence or absence of BMSCs. Cell proliferation was assessed using [ $^3$ H]-thymidine uptake assay. (D) BCWM.1 cells were cultured with control media in the absence and presence of IL-6 (25 ng/mL) and treated with enzastaurin (5 and 10  $\mu$ M) for 48 hours. Inhibition of proliferation was assessed by thymidine uptake assay. All data represent mean ( $\pm$  SD) of triplicate experiment.

not shown). The fraction affected (FA) and combination index (CI) are summarized as a table for each combination (Table 1).

#### Enzastaurin inhibited human WM cell growth in vivo

Finally, we evaluated the in vivo efficacy of enzastaurin using a xenograft mouse model of human WM. There was no significant

difference in the size of the tumors between the control and treated groups at baseline (volume in the treatment group = 50 mm $^3$  and volume in the control group = 34 mm $^3$ ,  $P$  = NS). Enzastaurin 80 mg/kg twice a day was given as previously described.<sup>10</sup> Serial caliper measurements of perpendicular diameters were done once a week to calculate tumor volume. Enzastaurin significantly reduced

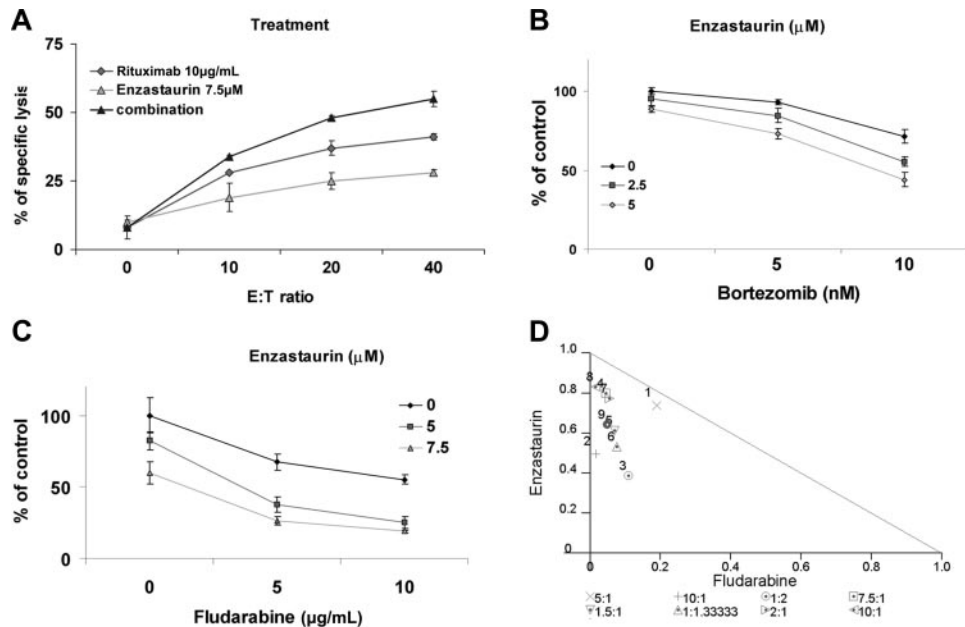


**Figure 6. Enzastaurin-induced cytotoxicity is enhanced in combination with the novel agent bortezomib, the anti-CD20 monoclonal antibody, rituximab, and fludarabine.** (A) ADCC realized on BCWM.1. BCWM.1 cells were treated with enzastaurin (7.5  $\mu$ M), rituximab (10  $\mu$ g/mL), and the combination in absence and presence of activated effector cells. Results are reported in terms of mean percentage of specific lysis characterized by measurement of release of calcein-AM upon different effector-target ratios (E/T ratio). The following controls showed minimum released of calcein-AM and were not added to the figure: medium alone, BCWM.1 or activated effector cells alone, BCWM.1 incubated with activated effector cells in absence of rituximab, activated effector cells with rituximab in absence of target cells. (B) BCWM.1 cells were cultured with enzastaurin (2.5 and 5  $\mu$ M) in the absence and presence of bortezomib (5 and 10 nM). Cytotoxicity was assessed with MTT assay. (C) BCWM.1 cells were cultured with enzastaurin (5 and 7.5  $\mu$ M) in the absence and presence of fludarabine (5 and 10  $\mu$ g/mL). Cytotoxicity was assessed with MTT assay. (D) Representative isobologram of enzastaurin associated to fludarabine with CalcuSyn software demonstrating synergy for the combinations 1 to 4: (1) enzastaurin 5  $\mu$ M plus fludarabine 5  $\mu$ g/mL; (2) enzastaurin 7.5  $\mu$ M plus fludarabine 5  $\mu$ g/mL; (3) enzastaurin 5  $\mu$ M plus fludarabine 10  $\mu$ g/mL; (4) enzastaurin 7.5  $\mu$ M plus fludarabine 10  $\mu$ g/mL.

**Table 1. Fraction affected (FA) and combination index (CI) of enzastaurin in combination with bortezomib, fludarabine, and dexamethasone**

Combination, dose	FA	CI
<b>Enzastaurin, <math>\mu</math>M/bortezomib, nM</b>		
2.5/5	0.15	1.072
2.5/10	0.45	0.838
5/5	0.27	0.921
5/10	0.56	0.757
<b>Enzastaurin, <math>\mu</math>M/fludarabine, <math>\mu</math>g/mL</b>		
5/5	0.62	0.676
7.5/5	0.74	0.695
5/10	0.77	0.524
7.5/10	0.81	0.63
<b>Enzastaurin, <math>\mu</math>M/dexamethasone, nM</b>		
7.5/50	0.42	0.895
10/50	0.71	0.969
7.5/100	0.45	0.877
10/100	0.74	0.945

All experiments were repeated at least twice.

WM tumor growth (Figure 7A) and increased survival (Figure 7B), compared to control animals treated with vehicle only. Comparisons of tumor volumes at 6 weeks following tumor implantation showed statistically significant differences across treatment groups ( $P = .028$ ). Assessing overall survival (OS), all the control mice were dead of tumor progression, whereas 67% (6/9) of treated mice remained alive at week 13. Using Kaplan-Meier curves and log-rank analysis, the mean OS was 56 days (95% confidence interval [CI], 42-70 days) in the control cohort versus 77 days (95% CI, 63-90 days) in the enzastaurin-treated group (log rank = 5.29;  $P = .022$ ) (Figure 7B). Of importance, there was no toxicity observed in the treated group. Whole tumor cell lysates from control and enzastaurin-treated mice were subjected to Western blotting to assess *in vivo* phosphorylation of Akt and GSK3 $\beta$ , which reflects PKC $\beta$  activity.<sup>10</sup> As shown in Figure 7C, enzastaurin induced significant inhibition of Akt and GSK3 $\beta$  phosphorylation in tumor cells *in vivo*.

## Discussion

The molecular pathways dysregulated in WM have not been well defined, and most of the therapeutic agents used in WM have been

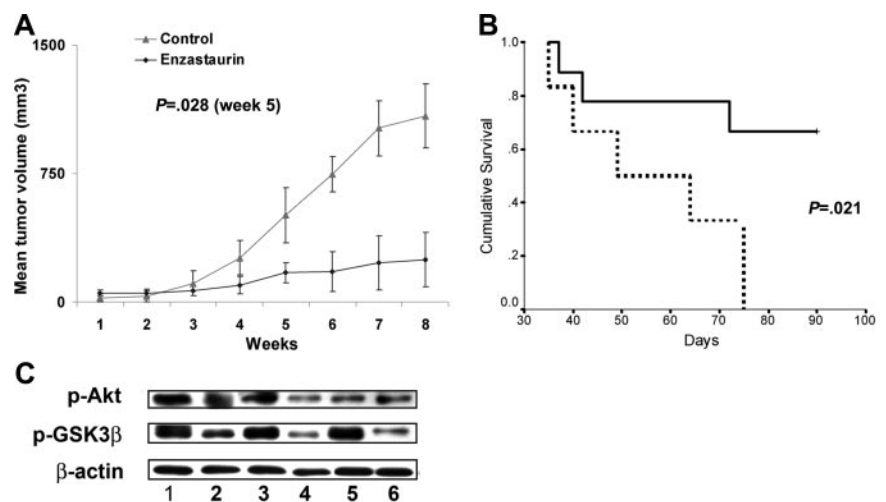
applied based upon their activity in other closely related lymphoproliferative disorders. Therefore, there is an urgent need to identify dysregulated molecular pathways in WM and then to develop targeted therapies. In this study, we demonstrate for the first time that PKC $\beta$  is overexpressed in WM cell lines and patient cells and that PKC $\beta$  signaling mediates WM survival and proliferation. Using PKC $\beta$  knockdown WM cells, we demonstrated that PKC $\beta$  is essential for the survival of WM cells.

We then studied the effect of the PKC $\beta$  inhibitor enzastaurin on WM cell growth and signaling *in vitro* and *in vivo*. Enzastaurin is an acyclic bisindolylmaleimide derived from staurosporine and acts as an ATP competitor. It interacts with protein kinase C, thereby modulating signal transduction pathways mediating tumor cell survival and proliferation.<sup>10</sup> The exact mechanism of action of enzastaurin is not well defined. It is not completely specific to PKC $\beta$  as it inhibits several kinases including novel and atypical PKCs.<sup>10</sup> It has demonstrated significant *in vitro* and *in vivo* cytotoxicity in B-cell malignancies, as well as in colon cancer and glioblastomas.<sup>10,24</sup> We demonstrated that enzastaurin inhibited proliferation and induced apoptosis in WM cell lines and in patient samples. In contrast, enzastaurin had no effect on normal mononuclear cells or growth of hematopoietic progenitor cells, suggesting a favorable therapeutic index. Enzastaurin activated both the intrinsic and extrinsic pathways of apoptosis resulting in caspase-8, caspase-9, and caspase-3 cleavage.

We next demonstrated that enzastaurin inhibited phosphorylation of PKC family members, and particularly phosphorylation of PKC $\beta$ , as well as downstream signaling proteins including p-Akt, p-GSK3 $\beta$ , and phospho-ribosomal protein S6. These data are consistent with previous studies demonstrating that enzastaurin inhibits both the PKC and PI3K/Akt pathways.<sup>10,24</sup> Furthermore, we showed that enzastaurin induced ERK phosphorylation in response to Akt inhibition, as previously described.<sup>17</sup> Since the MAPK ERK is a major signaling protein that regulates proliferation in many malignant cells, ERK activation might play a potential role in resistance to enzastaurin. We therefore tested the effect of the MEK inhibitor U0126 in combination with enzastaurin, and demonstrated that inhibition of ERK significantly enhances cytotoxicity of enzastaurin, indicating a potential role of combination of ERK and PKC inhibitors in future clinical trials.

The role of the bone marrow microenvironment in regulation of growth and drug resistance of malignant cells in WM is not well

**Figure 7. Enzastaurin inhibits human WM cell growth *in vivo*.** (A) Mean tumor volume in the mice treated with enzastaurin (80 mg/kg twice daily) (●) or with vehicle (dextrose 5% in water twice daily) (△). Error bars indicate the variation of tumor size between mice in each group. (B) Kaplan-Meier survival curve. Enzastaurin increased survival in the treated group (solid line,  $n = 9$ ) compared to the control group treated with vehicle only (dotted line,  $n = 6$ ) ( $P = .022$ ). (C) Tumor tissues from mice treated with control vehicle ( $n = 3$ , rows 1, 2, 3) or daily enzastaurin ( $n = 3$ , rows 4, 5, 6) were harvested, processed, and subjected to Western blotting using anti-p-Akt (ser473), anti-p-GSK3 $\beta$ , and anti- $\beta$ -actin antibodies.





defined. Previous studies in other B-cell malignancies have demonstrated that cytokines such as IL-6 and binding of tumor cells to BM stromal cells are critical regulators of tumor growth and conventional drug resistance. In this study, we showed that adherence to BM stromal cells and cytokines induce proliferation in WM cells, and importantly that enzastaurin induces cytotoxicity even in the bone marrow milieu.

The regulation of signaling pathways in malignant cells is complex, and therefore rationally designed combination of novel agents that target specific dysregulated pathways in WM is essential to overcome resistance and induce apoptosis. Therefore, we tested the effect of enzastaurin combined to other agents that are active against WM, such as the fludarabine, the anti-CD20 antibody rituximab,<sup>3</sup> and the proteasome inhibitor bortezomib.<sup>25</sup> We demonstrated that enzastaurin enhanced rituximab, bortezomib, fludarabine, and dexamethasone antitumor activity, suggesting that combining these agents may be therapeutically useful. Finally, we demonstrated that enzastaurin inhibited the growth of tumor WM cells *in vivo* in a SCID subcutaneous tumor model, further supporting this view.

In summary, we demonstrated that PKC family members are overexpressed in WM; and conversely, that the PKC $\beta$  inhibitor, enzastaurin, induces apoptosis and growth inhibition *in vitro* and *in vivo* in WM cells. In addition, enzastaurin can overcome conventional drug resistance and WM cell proliferation induced by the bone marrow microenvironment. Of most importance, the combina-

tion of enzastaurin with other novel therapeutic agents mediates synergistic WM cytotoxicity. Together, these studies provide the framework for clinical studies of enzastaurin, alone or in combination, to improve patient outcome in WM.

## Acknowledgments

This work was supported in part by the Leukemia and Lymphoma Research Foundation, the Multiple Myeloma Research Foundation, an ASH Scholar Award, the Bing Center for Waldenström Macroglobulinemia, and “la fondation pour la recherche médicale.” I.M.G. is a Lymphoma Research Foundation Scholar.

## Authorship

Contribution: A.-S.M., K.P., S.P.T., T.H., K.C.A., and I.M.G. designed the research, performed research, analyzed the data, and wrote the paper; X.J., H.T.N., G.O., Y.A., J.D., S.L.-K., E.H., M.S.R., and L.X. performed research; X.L., A.L., J.K., J.D., and S.L.-K. analyzed the data.

Conflict-of-interest disclosure: The authors declare no competing financial interests.

Correspondence: Irene M. Ghobrial, Medical Oncology, Dana-Farber Cancer Institute, 44 Binney St, Mayer 548A, Boston, MA, 02115; e-mail: irene\_ghobrial@dfci.harvard.edu.

## References

- Ghobrial IM, Gertz MA, Fonseca R. Waldenstrom macroglobulinaemia. *Lancet Oncol*. 2003;4:679-685.
- Owen RG, Treon SP, Al-Katib A, et al. Clinicopathological definition of Waldenstrom's macroglobulinemia: consensus panel recommendations from the Second International Workshop on Waldenstrom's Macroglobulinemia. *Semin Oncol*. 2003;30:110-115.
- Treon SP, Gertz MA, Dimopoulos M, et al. Update on treatment recommendations from the Third International Workshop on Waldenstrom's macroglobulinemia. *Blood*. 2006;107:3442-3446.
- Gertz MA, Anagnostopoulos A, Anderson K, et al. Treatment recommendations in Waldenstrom's macroglobulinemia: consensus panel recommendations from the Second International Workshop on Waldenstrom's Macroglobulinemia. *Semin Oncol*. 2003;30:121-126.
- Goekjian PG, Jirousek MR. Protein kinase C inhibitors as novel anticancer drugs. *Expert Opin Investig Drugs*. 2001;10:2117-2140.
- Shipp MA, Ross KN, Tamayo P, et al. Diffuse large B-cell lymphoma outcome prediction by gene-expression profiling and supervised machine learning. *Nat Med*. 2002;8:68-74.
- Hans CP, Weisenburger DD, Greiner TC, et al. Expression of PKC-beta or cyclin D2 predicts for inferior survival in diffuse large B-cell lymphoma. *Mod Pathol*. 2005;18:1377-1384.
- Abrams ST, Lakum T, Lin K, et al. B-cell receptor signalling in chronic lymphocytic leukemia cells is regulated by overexpressed active protein kinase C $\beta$ . Prepublished on September 26, 2006, as DOI 10.1182/blood-2006-03-012021. (Now available as *Blood*. 2007;109:1193-1201.)
- Podar K, Tai YT, Davies FE, et al. Vascular endothelial growth factor triggers signaling cascades mediating multiple myeloma cell growth and migration. *Blood*. 2001;98:428-435.
- Graff JR, McNulty AM, Hanna KR, et al. The protein kinase C $\beta$ -selective inhibitor, Enzastaurin (LY317615.HCl), suppresses signaling through the AKT pathway, induces apoptosis, and suppresses growth of human colon cancer and glioblastoma xenografts. *Cancer Res*. 2005;65:7462-7469.
- Podar K, Raab MS, Zhang J, et al. Targeting PKC in multiple myeloma: *in vitro* and *in vivo* effects of the novel, orally available small-molecule inhibitor enzastaurin (LY317615.HCl). Prepublished on October 5, 2006, as DOI 10.1182/blood-2006-08-042747. (Now available as *Blood*. 2007;109:1669-1677.)
- Keyes KA, Mann L, Sherman M, et al. LY317615 decreases plasma VEGF levels in human tumor xenograft-bearing mice. *Cancer Chemother Pharmacol*. 2004;53:133-140.
- Santos D HA, Tournilhac O, Leleu X, et al. Establishment of a Waldenstrom's macroglobulinemia cell line (BCWM.1) with productive *in vivo* engraftment in SCID-hu mice. *Blood*. 2005;106:288a. Abstract 979.
- Al-Katib AM, Mensah-Osman E, Aboukameel A, Mohammad R. The Wayne State University Waldenstrom's macroglobulinemia preclinical model for Waldenstrom's macroglobulinemia. *Semin Oncol*. 2003;30:313-317.
- Ghobrial IM, McCormick DJ, Kaufmann SH, et al. Proteomic analysis of mantle-cell lymphoma by protein microarray. *Blood*. 2005;105:3722-3730.
- Tassone P, Neri P, Kutok JL, et al. A SCID-hu *in vivo* model of human Waldenstrom macroglobulinemia. *Blood*. 2005;106:1341-1345.
- Hideshima T, Catley L, Yasui H, et al. Perifosine, an oral bioactive novel alkylphospholipid, inhibits Akt and induces *in vitro* and *in vivo* cytotoxicity in human multiple myeloma cells. Prepublished on January 17, 2006, as DOI 10.1182/blood-2005-08-3434. (Now available as *Blood*. 2006;107:4053-4062.)
- Dillon CP, Sandy P, Nencioni A, Kissler S, Rubinson DA, Van Parijs L. Rnai as an experimental and therapeutic tool to study and regulate physiological and disease processes. *Annu Rev Physiol*. 2005;67:147-173.
- Rubinson DA, Dillon CP, Kwiatkowski AV, et al. A lentivirus-based system to functionally silence genes in primary mammalian cells, stem cells and transgenic mice by RNA interference. *Nat Genet*. 2003;33:401-406.
- Tai YT, Li X, Tong X, et al. Human anti-CD40 antagonist antibody triggers significant antitumor activity against human multiple myeloma. *Cancer Res*. 2005;65:5898-5906.
- Hatzimichael EC, Christou L, Bai M, Kolios G, Kefala L, Bourantas KL. Serum levels of IL-6 and its soluble receptor (sIL-6R) in Waldenstrom's macroglobulinemia. *Eur J Haematol*. 2001;66:1-6.
- Mitsiades CS, Mitsiades NS, Munshi NC, Richardson PG, Anderson KC. The role of the bone microenvironment in the pathophysiology and therapeutic management of multiple myeloma: interplay of growth factors, their receptors and stromal interactions. *Eur J Cancer*. 2006;42:1564-1573.
- Tassone P, Neri P, Carrasco DR, et al. A clinically relevant SCID-hu *in vivo* model of human multiple myeloma. *Blood*. 2005;106:713-716.
- Querfeld C, Rizvi MA, Kuzel TM, et al. The selective protein kinase C beta inhibitor enzastaurin induces apoptosis in cutaneous T-cell lymphoma cell lines through the AKT pathway. *J Invest Dermatol*. 2006;126:1641-1647.
- Dimopoulos MA, Anagnostopoulos A. Waldenstrom's macroglobulinemia. *Best Pract Res Clin Haematol*. 2005;18:747-765.